Asian Journal of Chemistry; Vol. 33, No. 1 (2021), 240-244

ASIAN JOURNAL OF CHEMISTRY

https://doi.org/10.14233/ajchem.2021.22996

Photocatalytic Activity of Nickel Doped CoO Nanocomposite for the Degradation of Azure A Dye

NIRMAL SINGH*, AVINASH KUMAR RAI, RITU VYAS and RAMESHWAR AMETA

Department of Chemistry, PAHER University, Udaipur-313003, India

*Corresponding author: E-mail: nirmalsingh0068@gmail.com

Received: 24 September 2020; *Accepted*: 17 November 2020; *Published online*: 10 December 2020; AJC-20204

Nanocrystalline cobalt(II) oxide doped with nickel was prepared using the sol-gel method and employed as a photocatalyst for azure A dye degradation under visible light. The prepared photocatalyst was analyzed using energy-dispersive X-ray (EDX) spectroscopy, field emission scanning electron microscopy (FESEM), Fourier-transform infrared (FTIR), X-ray diffraction (XRD) and high-resolution transmission electron microscopy (HRTEM). The photocatalytic activity of Ni-doped CoO under different working parameters, like concentration, pH, dosage (Ni-doped and undoped CoO), light intensity for the degradation of azure A dye was also optimzed. It was observed that the dye degradation rate improved after doping. Approximately 76% and 85% of azure A dye was degraded within 90 min through undoped and Ni-doped CoO, respectively.

Keywords: Azure A dye, Nanocrystalline, Nickel, Cobalt(II) Oxide, Sol-gel technique, Photocatalyst.

INTRODUCTION

Presently, water pollution has become a serious concern for all living beings. All the pollutants whether inorganic or organic present in the wastewater from industries poses a great concern and needs treatment of wastewater. The sources of these pollutants are generally chemical, textile and drug manufacturing industries. The wastewater contains several types of pollutants such as organic dyes, pharmaceutical ingredients, fertilizers, pesticides, phenols, surfactants, organohalides, *etc*. Therefore, treatments of such polluted water are necessary. Normally, the wastewater consists of 99.9 % water by weight, where as the remaining 0.1 % only present as suspended or dissolved materials. This solid material is a mixture of excrements, detergents, food leftovers, grease, oils, salts, plastics, heavy metals, sands, grits, *etc*. which affects the quality of water abnormally [1-3].

Various techniques based on nanomaterials are employed for water treatment [4]. In the advanced oxidation process (AOP), the applications of the semiconductors of metal oxides have received a considerable attention for dye wastewater treatment because of the low toxicity, good degradation efficiency and chemical and physical properties of metal oxides. Advanced oxidation process (AOP) is a procedure set of the green chemical treatments employed for the removal of inorganic and organic materials from wastewater through oxidation [5,6]. Transition metals and their composites and oxides have outstanding photocatalytic activities for organic pollutant degradation. Various binary semiconducting materials, such as ZnO, CuS, TiO_2, WO_3, SnO_2, CuO, ZnO, Al_2O_3 and CeO_2, which are based on metals are investigated and used as photocatalysts [7-11].

Farhadi *et al*. [12] synthesized $[Co(NH_3)_5(H_2O)](NO_3)_3$ complex (17.5 nm spherical shape) using thermal decomposition method with semiconductor properties. As-synthesized composite was used to degrade methylene blue under visible-light irradiation. Li and Chopra [13] synthesized a nanowire heterostructure of $[(Co_3O_4)(WO_3)]$ *via* a thermal oxidation method and utilized it's photocatalytic performance and behaviour for the degradation of organic water pollutants. It was revealed that the photocatalytic efficiency of the synthesized heterostructure nanowire was increased by ~30% as compared to as-produced Co_3O_4 nanowires. Kulsi *et al*. [14] synthesized Bi_2Se_3 and Ni doped Bi_2Se_3 *via* a solvothermal approach and reported the enhanced photocatalytic performance for the degradation of malachite green dye in comparison to pure Bi_2Se_3 in the presence of light.

Sedneva *et al*. [15] synthesized nanocomposites of oxides of titanium (IV) and cobalt (II) and evaluated photocatalytic

activity in presence of visible light attempted to correlate it with cobalt content and temperature. Subramanyam *et al*. [16] synthesized Ni doped CuS nanoparticles by wet chemical co-precipitation method using EDTA molecules as templates. They studied about photocatalytic degradation of rhodamine B dye as a model pollutant using as-synthesized bare and Ni doped CuS nanoparticles in presence of sunlight irradiation. It was found that doping of 3% Ni in CuS nanoparticles enhanced the degradation efficiency and 98.46% degradation could be achieved within 60 min of sunlight irradiation; while in case of bare CuS, it was only 83.22%. Santhi *et al*. [17] used microwave irradiation method to synthesize Ni-doped WO_3 and $NiWO_4$ nanomaterials. They investigated the effects of different rate affecting parameters for the degradation of alizarin red S dye and achieved 77 % degradation efficiency at the optimum conditions. Thus, applications of doped nanoparticles for removal of toxic and hazardous dyes is still of great importance. The aim of the present work is to synthesize Ni-doped CoO *via* sol gel method and utilized as a photocatalytic material for the degradation of azure A dye. This method has been chosen based on its advantages over some other synthesis methods as its low cost, simple method and high quality of synthesized Ni-doped CoO material.

EXPERIMENTAL

The chemicals used in this work *viz*. cobalt(II) chloride hexahydrate ($CoCl_2{\cdot}7H_2O$), nickel(II) chloride hexahydrate ($NiCl_2{\cdot}7H_2O$), sodium carbonate (anhydrous) were of analytical grade (99.9%). Azure A dye was purchased from Himedia Chemicals (CAS No. 531-53-3). All the solutions were prepared in double distilled water.

Synthesis of photocatalyst (Ni doped $CoCl_2$): Freshly prepared cobalt chloride (0.1 M) and sodium carbonate (0.1 M) solutions were mixed with continuous stirring, until the purple color gel formed. The gel was washed with double distilled water and filtered, then dried in an oven at 100 ºC for 24 h [18].

In the next step, freshly prepared nickel(II) chloride (0.1 M) and prepared CoO (0.1 M) were mixed using magnetic stirring for 30 min. An obtained coloured gel was washed and filtered with double distilled water. This gel was dried in an oven at 100 ºC for 4 h, which resulted in the formation of a black colour nickel-cobalt oxide.

RESULTS AND DISCUSSION

Field emission scanning electron microscopy (FESEM): Fig. 1 illustrates the morphology of Ni doped CoO nanocomposite obtained through the FESEM analysis, which shows the presence of a spherical structure.

EDX analysis: The data obtained through EDX spectroscopy showed the presence of 0.33%, 39.95% and 59.72% for Ni, Co, O, respectively, without any impurities.

XRD analysis: The patterns of X-ray diffraction (X.Pert Pro.) were acquired for Ni doped CoO nanocomposites. The Debye-Scherrer equation (eqn. 1) was used to calculate the particle size of the synthesized nanocomposite.

$$D = \frac{0.9\lambda}{B\cos\theta} \quad (1)$$

where, B = FWHM and λ = X-ray wavelength (CuKα radiation 1.54 Å). At 2θ value, different particle size of synthesized nanocomposite materials were obtained (Table-1). The average size of the synthesized photocatalyst was found to be ~19.08 nm.

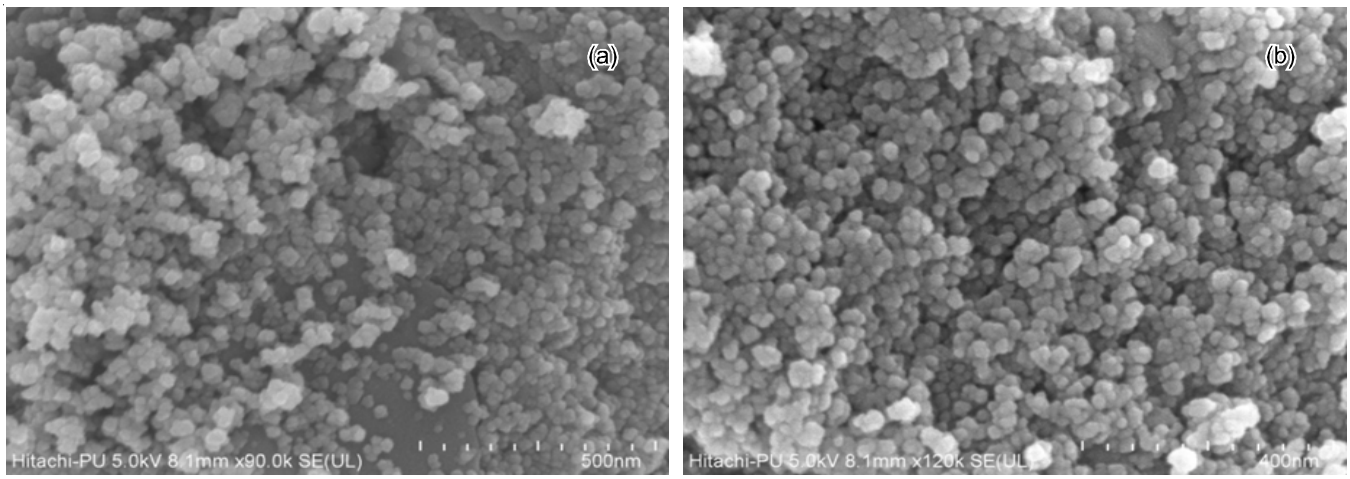

Fig. 1. FESEM image of Ni-doped CoO

TABLE-1
PARTICLE SIZE OF NICKEL DOPED CoO AT 2θ VALUE

Pos. [°2θ]	FWHM Total [°2θ]	d-spacing [Å]	Rel. intensity [%]	Area [cts*°2θ]	Particle size (nm)	Average particle size (nm)
31.2395	0.5442	2.86089	24.96	75.78	15.82	
36.8240	0.3246	2.43883	100.00	187.35	26.92	
44.7240	0.8575	2.02467	27.19	145.14	10.46	19.08
59.3130	0.5116	1.55679	25.51	63.81	18.65	
65.1539	0.4177	1.43063	38.51	79.01	23.56	

FTIR analysis: In the FTIR spectrum of Ni doped CoO nanocomposite, a broad band was observed at 3430.3 cm^{-1} which is attributed due to coordinated/entrapped water stretching vibrations. The other bands appeared at 662 and 569 cm^{-1} correspond to the bending modes of cobalt oxide and nickel oxide vibrations, respectively [19].

HRTEM analysis: HRTEM images (The Tecnai G2 20 (FEI) S-Twin 200 kV transmission electron microscope.) were taken in order to determine the shape and size of nanocrystalline Ni doped CoO material. It is seen that the nanocrystals are more or less cubic and particle size is 13.2 nm. From Fig. 2, it is clear that the no agglomeration of nanoparticles takes place and morphology seems to be indexed on cubic, spinel structure of the nanocomposite.

Photocatalytic degradation study: By dissolving azure A dye (0.0291 g) in 100 mL double distilled water, a stock solution of azure A dye (1×10^{-3} M) was obtained. Then, the aliquot solutions were prepared from the stock solution. At λ_{max} = 630 nm, the absorbance of the solution of azure A dye was determined. Control experiments were performed, and the presence of both light energy and nickel-cobalt oxide is essential for azure A dye degradation, which proved that the nature of azure A degradation is photocatalytic. After the addition of 0.1 g of nanocomposite (Ni doped CoO) to 50 mL of dye solution (2.8×10^{-5} M), the photocatalytic degradation of azure A dye was investigated. Using a tungsten lamp of 200 W (Philips), the reaction mixture was subjected to visible light. Solution absorbance was determined at different time intervals by using a spectrophotometer (Systronics Model 106). Light intensity was changed by varying the distance of the reaction mixture from the light source. The pH solution was adjusted with standardized 0.1 N NaOH and/or HCl solutions.

An obtained plot of log A *versus* time exhibited a straight line, indicating that the photocatalytic degradation of azure A dye followed pseudo-first order kinetics. The rate constant for degradation of dye was calculated by the following equation:

$$k = 2.303 \times \text{slope} \quad (2)$$

A typical run was obtained for the photocatalytic degradation of azure A dye by employing Ni doped CoO photocatalyst (Table-2), where all the parameters were optimized.

TABLE-2
TYPICAL RUN
pH = 8.0, [Azure A] = 2.8×10^{-5} M, Amount of composite = 0.10 g , Light intensity = 60.0 mW cm^{-2}

Time (min)	Ni-CoO		CoO	
	Absorbance (A)	1 + log A	Absorbance (A)	1 + log A
0	0.605	0.7818	0.603	0.7803
10	0.512	0.7093	0.523	0.7185
20	0.409	0.6117	0.441	0.6444
30	0.330	0.5185	0.376	0.5752
40	0.271	0.4330	0.327	0.5145
50	0.233	0.3674	0.270	0.4314
60	0.190	0.2788	0.232	0.3655
70	0.159	0.2014	0.186	0.2695
80	0.131	0.1173	0.156	0.1931
90	0.102	0.0086	0.140	0.1461

Rate constant (k) Ni-CoO = 3.29×10^{-4} s^{-1}, Rate constant (k) CoO = 2.01×10^{-4} s^{-1}

Effect of working parameters

pH variation: The effects of pH variation in the range of 5.5-9.5 were studied. The degradation rate increased with an increase in pH up to 8; however, this rate decreased with the further increase in pH (Fig. 3). The reason is attributed due to the dissolved oxygen abstracted an electron from the conduction band to produce $O_2^{\bullet -}$. The photocatalytic degradation rate of the dye may be increased because of the availability of excess $^{\bullet}OH$ radicals and $O_2^{\bullet -}$ anions. The photocatalytic degradation rate of the dye may be decreased because the dye was exhibited the anionic form, which experienced repulsion force with a negatively charged surface of composites because of the absorption of numerous OH^- ions on the composite surface. The composite was active from nearly neutral to slightly basic pH range.

Variation of dye concentraion: In the dye concentration range of 2.2×10^{-5}-3.4×10^{-5} M, an influence of the dye concentration was observed on the photocatalytic degradation of

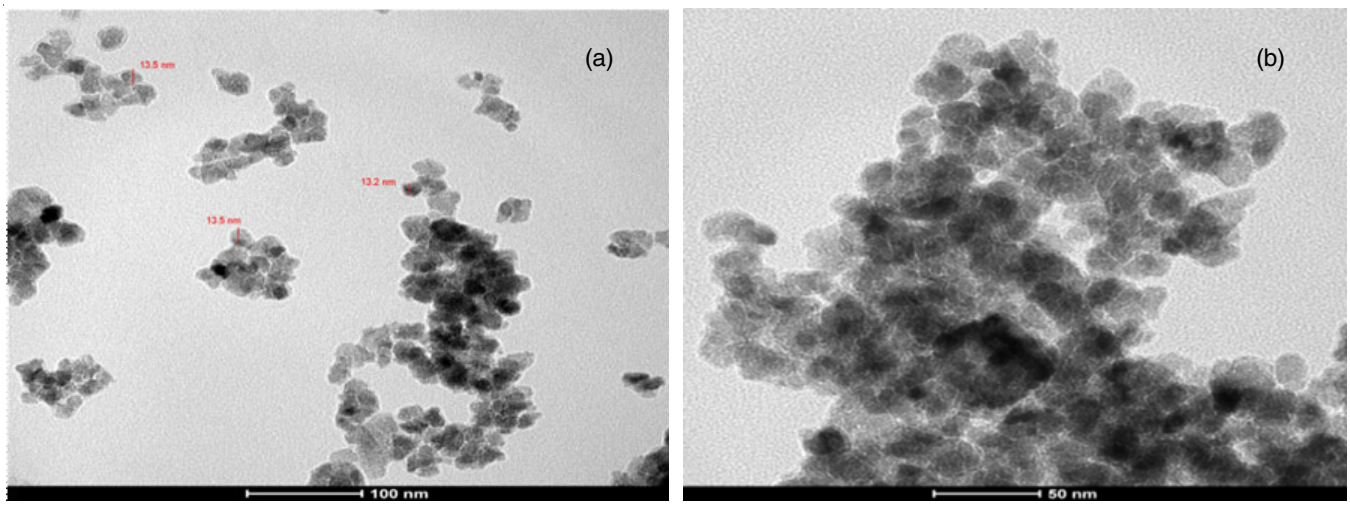

Fig. 2. HRTEM image of Ni-dopped CoO

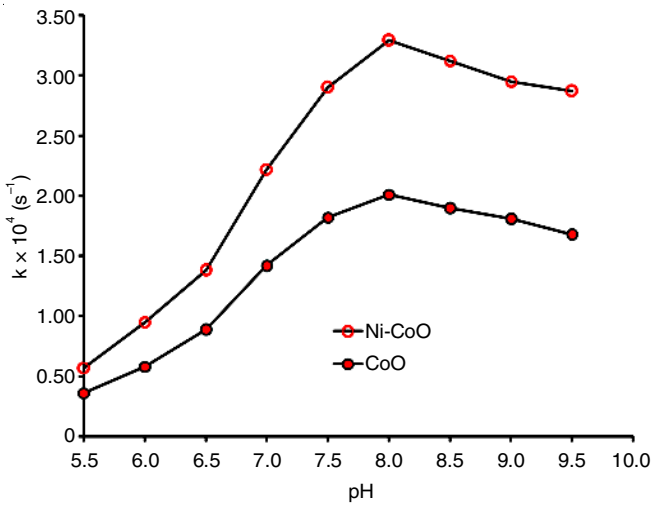

Fig. 3. Effect of variation of pH

azure A dye. It is observed that with an increase in the dye concentration, the dye degradation rate increased because many dye molecules became available for energy transfer and excitation (Fig. 4). However, when the concentration exceeds 2.8×10^{-5} M, the photocatalytic degradation exhibited a decreasing trend because dye molecules started behaving as a filter for incident light and prevented the desired light intensity from reaching to composite particles, thereby leading to a decrease in the photocatalytic degradation rate of the dye.

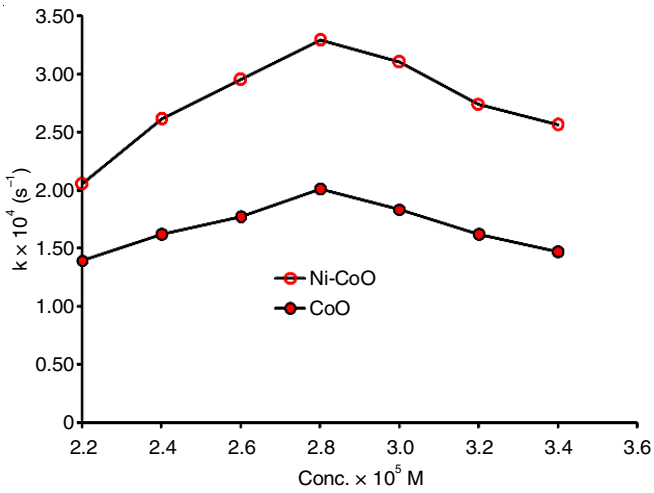

Fig. 4. Effect of variation of dye concentration

Effect of dosage: The effect of the dosage variation of the nanocomposite on the dye degradation rate was investigated in the range of 0.02-0.140 g. With an increase in the photocatalyst amount, the photocatalytic degradation rate increased (Fig. 5). At 0.10 g of nanocomposite, the degradation rate was maximum because the surface area was exposed increased. However, after a limit, with a further increase in the dosage, no increase was observed in the area of the exposed surface of the photocatalyst. Multilayers were formed, which made e^--h^+ combination highly probable, thus the degradation rate decreased.

Effect of light intensity variation: An influence of light intensity on photocatalytic degradation was investigated by

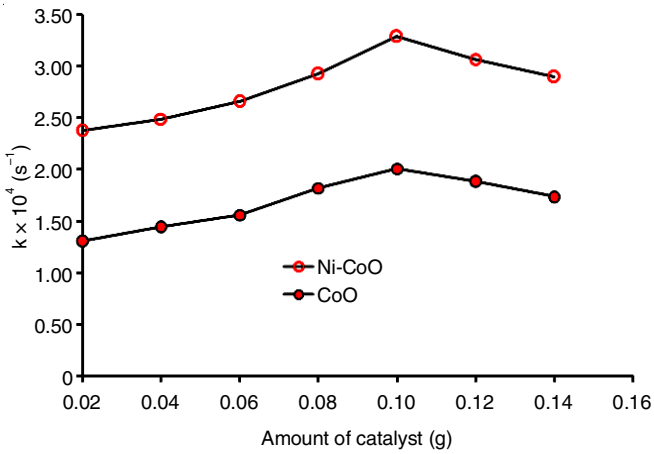

Fig. 5. Effect of variation of amount of the composite

changing the intensity in 20-70 mW cm^{-2} range. The photocatalytic degradation of azure A dye exhibited an increasing tend with the light intensity, an increase in the number of photons that struck per unit area of the photocatalyst surface per unit time (Fig. 6). For azure A dye degradation, the maximum rate was obtained at 60 mW cm^{-2}. Some thermal side reactions also occurred at higher light intensities; thus, the photocatalytic degradation rate slightly decreased when the light intensity further increased.

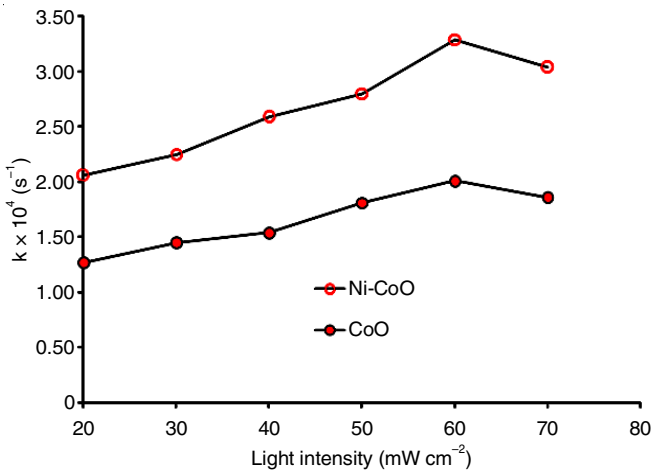

Fig. 6. Effect of variation of light intensity

Comparison with reported catalysts: Table-3 presents the comparison of performance of Ni-doped cobalt(II) oxide with other reported photocatalytic materials for the degradataion of azure A dye. The Ni-doped cobalt(II) oxide exhibited a high efficiency of azure A dye degradation of 85% after 90 min. This comparison indicated an excellent performance of Ni-doped cobalt(II) oxide and can be utilized as promising material for actual applications like environmental remediation.

Mechanism

On the basis of observed experimental conditions, a tentative mechanism for the photocatalytic degradation of azure A dye, using Ni-doped CoO composite as photocatalyst has been proposed. Electrons in Ni-doped CoO are excited to its conduction band on light irradiation. The •OH radical participates

TABLE-3
COMPARISON OF PERFORMANCE OF Ni DOPED COBALT(II) OXIDE AGAINST AZURE A DYE WITH THE RECENTLY REPORTED PHOTOCATALYSTS

Name of catalyst	Experimental condition (conc., pH, amount of catalyst)	% of Degradation/Removal (time)	Ref.
Carbon doped ZnO	[Azure A]= 4.2×10^{-5} M, pH=10, [catalyst] = 60 mg	53.75 % (60 min)	[20]
N doped ZnO	[Azure A]= 1.6×10^{-5} M, pH=8.0, [catalyst] = 100 mg	61.23 % (40 min)	[21]
$BaCrO_4$	[Azure A]= 3.0×10^{-5} M, pH=9.0, [catalyst] = 60 mg	65.92 % (135 min)	[22]
Sanil shell (Rostellaria) powder	[Azure A]= 5 mg l^{-1}, pH= 10, [catalyst] = 60 mg	79 % (30 min)	[23]
$BaCrO_4$	[Azure A]= 5.0×10^{-5} mol dm^{-3}, pH= 10, [catalyst] = 200 mg	99 % (90 min)	[24]
Ni-CoO	[Azure A]= 2.8×10^{-5} M, pH=8.0, [catalyst] = 100 mg	85 % (90 min)	Present work

as an active oxidizing species and confirmed by using hydroxyl radical scavenge (2-propanol) where, the rate of degradation was found to decrease. Thus, a tentative mechanism for photocatalytic degradation of azure A dye may be proposed as:

$$^1\text{Azure A}_0 \xrightarrow{hv} {}^1\text{Azure A}_1 \quad (3)$$

$$^1\text{Azure A}_1 \xrightarrow{ISC} {}^3\text{Azure A}_1 \quad (4)$$

$$\text{Ni-CoO} \xrightarrow{hv} \text{Ni-CoO } [h^+ (VB) + e^- (CB)] \quad (5)$$

$$h^+ + OH^- \longrightarrow {}^\bullet OH \quad (6)$$

$$^3\text{Azure A}_1 + {}^\bullet OH \longrightarrow \text{Leuco Azure A} \quad (7)$$

$$\text{Leuco Azure} \longrightarrow \text{A Products} \quad (8)$$

Azure A dye molecule absorbed the suitable wavelength light and was excited to the first excitation singlet state and then through intersystem crossing to the triplet state. By contrast, the Ni-doped CoO photocatalyst utilizes the incident light energy for exciting its electrons to the conduction band from the valence band, thereby leaving a hole behind. The h^+ hole reacts with the ^-OH ion present in the aqueous solution to produce $^\bullet OH$ radicals. These radicals react with azure A dye and converted it into the unstable leuco form, which ultimately degrades into smaller components.

Conclusion

The Ni doped CoO nanocomposite was prepared successfully by sol-gel method. The nanostructure of composite sample was characterized by FESEM, XRD, FTIR and HRTEM. The results showed that best degradation efficiency of azure A dye (85%) was achieved at the optimum conditions of pH 8.0, concentration (2.8×10^{-5} M), dosage (0.10 g) and light intensity (60 mW cm^{-2}). Moreover, Ni doped CoO nanocomposite exhibited a higher efficiency of photodegradation of azure A dye compared to other reported similar materials.

ACKNOWLEDGEMENTS

The authors are thankful to Prof. S.C. Ameta, Department of Chemistry, PAHER University, Udaipur for their help in the course of this work and to SAIF, CIL, Chandigarh, India for FESEM, EDS & XRD; and IIT Delhi for HRTEM analysis.

CONFLICT OF INTEREST

The authors declare that there is no conflict of interests regarding the publication of this article.

REFERENCES

1. R. Gusain, K. Gupta, P. Joshi and O.P. Khatri, *Adv. Colloid Interface Sci.*, **272**, 102009 (2019); https://doi.org/10.1016/j.cis.2019.102009
2. N.F. Gray, Water Technology: An Introduction for Environmental Scientists and Engineers, Elsevier Science & Technology Books: Amsterdam, The Netherlands, edn 2 (2005).
3. S.D. Lin, Water and Wastewater Calculations Manual, McGraw-Hill Companies, Inc.: New York, USA, edn 2 (2007).
4. X.Y. Xue, R. Cheng, L. Shi, Z. Ma and X. Zheng, *Environ. Chem. Lett.*, **15**, 23 (2017); https://doi.org/10.1007/s10311-016-0595-x
5. S.H.S. Chan, T. Yeong Wu, J.C. Juan and C.Y. Teh, *J. Chem. Technol. Biotechnol.*, **86**, 1130 (2011); https://doi.org/10.1002/jctb.2636
6. G. Mamba and A. Mishra, *Catalysts*, **6**, 79 (2016); https://doi.org/10.3390/catal6060079
7. A. Gupta, J.R. Saurav and S. Bhattacharya, *RSC Adv.*, **5**, 71472 (2015); https://doi.org/10.1039/C5RA10456D
8. U.I. Gaya and A.H. Abdullah, *J. Photochem. Photobiol. Photochem. Rev.*, **9**, 1 (2008); https://doi.org/10.1016/j.jphotochemrev.2007.12.003
9. G. Wang, Z. Liu and X. Liu, *Chemistry Bull.*, **76**, 689 (2013) (In Chinese).
10. H. Khojasteh, M. Salavati-Niasari and S. Mortazavi-Derazkola, *J. Mater. Sci. Mater. Electron.*, **27**, 3599 (2016); https://doi.org/10.1007/s10854-015-4197-3
11. M.P.B. Vega, M. Hinojosa-Reyes, A. Hernández-Ramírez, J.L.G. Mar, V. Rodríguez-González and L. Hinojosa-Reyes, *J. Sol-Gel Sci. Technol.*, **85**, 723 (2018); https://doi.org/10.1007/s10971-018-4579-0
12. S. Farhadi, M. Javanmard and G. Nadri, *Acta Chim. Slov.*, **63**, 335 (2016); https://doi.org/10.17344/acsi.2016.2305
13. Y. Li and N. Chopra, *J. Catal.*, **329**, 514 (2015); https://doi.org/10.1016/j.jcat.2015.06.015
14. C. Kulsi, A. Ghosh, A. Mondal, K. Kargupta, S. Ganguly and D. Banerjee, *Appl. Surf. Sci.*, **392**, 540 (2017); https://doi.org/10.1016/j.apsusc.2016.09.063
15. T.A. Sedneva, M.L. Belikov, E.P. Lokshin and A.T. Belyaevskii, *Theor. Found. Chem. Eng.*, **50**, 498 (2016); https://doi.org/10.1134/S0040579516040278
16. K. Subramanyam, N. Sreelekha, D. Amaranatha Reddy, G. Murali, K. Rahul Varma and R.P. Vijayalakshmi, *Solid State Sci.*, **65**, 68 (2017); https://doi.org/10.1016/j.solidstatesciences.2017.01.008
17. K. Santhi, C. Rani and S. Karuppuchamy, *J. Mater. Sci. Mater. Electron.*, **27**, 5033 (2016); https://doi.org/10.1007/s10854-016-4390-z
18. N. Tharayil, R. Raveendran, A. Vaidyan and P. Chithra, *Indian J. Eng. Mater. Sci.*, **15**, 489 (2008).
19. N. Singh, M. Jangid, N. Shorgar and P. Tak, *Res. J. Chem. Environ.*, (2020) (in press).
20. R.P. Purnima, P. Tak and S. Benjamin, *Sci. Rev. Chem. Commun.*, **6**, 19 (2016).
21. P. Rathore, R. Ameta and S. Sharma, *J. Textile Sci. Technol.*, **1**, 118 (2015); https://doi.org/10.4236/jtst.2015.13013
22. S. Gupta, P. Tak, R. Ameta and S. Benjamin, *J. Adv. Chem. Sci.*, **1**, 38 (2015).
23. A. Muneer, R.Q. AL-Shemary and E.T. Kareem, *J. Int. Pharm. Res.*, **45**, 123 (2015).
24. B. Pare, D. Singh, V.S. Solanki, P. Gupta and S. Jonnalagadda, *Int. J. Chem.*, **3**, 351 (2014).